Solid State Communications, Vol. 68, No. 2, pp. 201-204, 1988.
Printed in Great Britain.

0038-1098/88 $3.00 + .00
Pergamon Press plc

Fe/Pd SECOND-ORDER SUPERLATTICES

A. Boufelfel, B. Hillebrands, G. I. Stegeman, and Charles M. Falco
Department of Physics and Optical Sciences Center
University of Arizona, Tucson, Arizona, U.S.A. 85721

(Received 3 August 1988 by A. A. Maradudin)

We report the structural and magnetic properties of a new class of Fe/Pd second-order superlattices, formed by alternating two bilayers with different repeat periods. Chemical and structural characterization were obtained using Rutherford backscattering spectroscopy (RBS) and several x-ray diffraction techniques, respectively. The properties of the collective spin wave spectrum were studied by Brillouin scattering.

Introduction

Metallic superlattices, in which at least one of the constituents is magnetic or superconducting in the bulk, have been the objects of increasing interest the past few years.[1] However, variations in physical quantities (such as magnetization, hyperfine field, resistivity, superconducting transition temperature, or elasticity) as a function of bilayer thickness, Λ, in many cases are not clearly understood. It is therefore of increasing importance to find new or improved methods of determining the physical properties of multilayered structures, as well as of studying new multilayered structural geometries.

In this communication, we report for the first time results on the preparation and characterization of a new class of Fe/Pd metallic multilayers for which we adopt the name "second-order" superlattice. This second-order superlattice consists of two alternating periods, Λ_1 and Λ_2. Here, $\Lambda_1 = m_1 d_{Fe} + n_1 d_{Pd}$, and $\Lambda_2 = m_2 d_{Fe} + n_2 d_{Pd}$, where m_1, m_2, n_1, and n_2 are integers, and d_{Fe}, and d_{Pd} are the atomic spacings in the growth direction for Fe and Pd respectively. The superlattice wavelength Λ is the sum of Λ_1 and Λ_2. For the samples reported here, this period was repeated approximately fifty times.

Sample Preparation

The samples were prepared using magnetically enhanced dc sputtering guns to deposit Fe and Pd. The sputtering system has been described elsewhere,[2] as has our technique for simultaneously growing several samples with different wavelengths.[3] With all relevant deposition parameters held constant (Ar pressure, plasma current and voltage, target current, and substrate table velocity), deposition rates are constant to better than ±0.3%. Typical deposition pressures are in the range 4 to 6 mTorr during sputtering and on the order of 5×10^{-8} Torr before and after sputtering. The samples were deposited on polished, single-crystal sapphire substrates with the c-axis in the plane.

The chemical composition of the samples was determined using Rutherford backscattering spectroscopy (RBS) with a 4.7-MeV $^4He^+$ ion beam.[4] The thickness ratio (Fe/Pd) was determined with a precision better than ±1%, and the absolute thickness of our samples to within ±5%. The upper limit on the oxygen content inside these samples was determined to be ~1%.

X-Ray Characterization

The structural coherence of the fabricated second-order superlattices was determined by several x-ray diffraction techniques. X-ray diffraction measurements in the θ-2θ configuration at both high angles and grazing incidence were used, as was a wide-film Debye-Scherrer camera. Figure 1 shows a typical θ-2θ spectrum for Sample A. The probing beam was $CuK_{\alpha_{1,2}}$ radiation (λ = 1.5418 Å).

At grazing incidence, we are able to simulate the reflectance as a function of the incident angle θ,[5,6] using the theoretical optical constants for bulk Fe and Pd as input parameters for the computations. The optical constants are calculated using the relations[7]

$$\delta = \frac{r_0\lambda^2 N}{2\pi}(f_0 + f') ,$$

$$k \equiv \beta = \frac{r_0\lambda^2 N}{2\pi} f'' = \frac{\lambda\mu}{4\pi} .$$

The refractive index is given by

$$\tilde{n} = 1 - \delta + ik ,$$

where N is the number density of atoms, μ is the linear absorption coefficient, r_0 is the classical electron radius, f' and f'' are the corrections to the atomic scattering angles, and f_0 is the atomic scattering factor in the high-energy limit.[7] In the case of CuK_α radiation, where the incident beam energy is relatively low and for small scattering angles ($2\theta \sim 1^0$ to 10^0), $f_0 \cong Z$, where Z is the atomic number. We used the tabulated corrections f' and f'' from Ref. 8 to obtain the results summarized in Table 1. These results are used as input parameters for our calculation of the angular dependence of the x-ray reflectivity.

Our previous studies of Fe/Pd superlattices showed that interdiffusion is limited to approximately two atomic layers.[9] For this reason, we did not include possible roughness and interdiffusion at the interfaces in our reflectivity calculations, but we did take into account the spatial variation of the deposition profile.[3] Shown in Table 2 are the values of the calculated and measured peak positions in the range $2\theta = 1.5^0$ to 4.2^0 for two Fe/Pd samples. The total number of periods for Sample A is 51, and for Sample B it is 50. In Table 2, n is the peak order, and $2\theta_0$ and $2\theta_c$ are the observed and the calculated peak positions, respectively. Considering the possible uncertainties in the calculated optical constants attributable to deviations from bulk densities for Fe and Pd, as well as the uncertainties in f' and f'' noted by

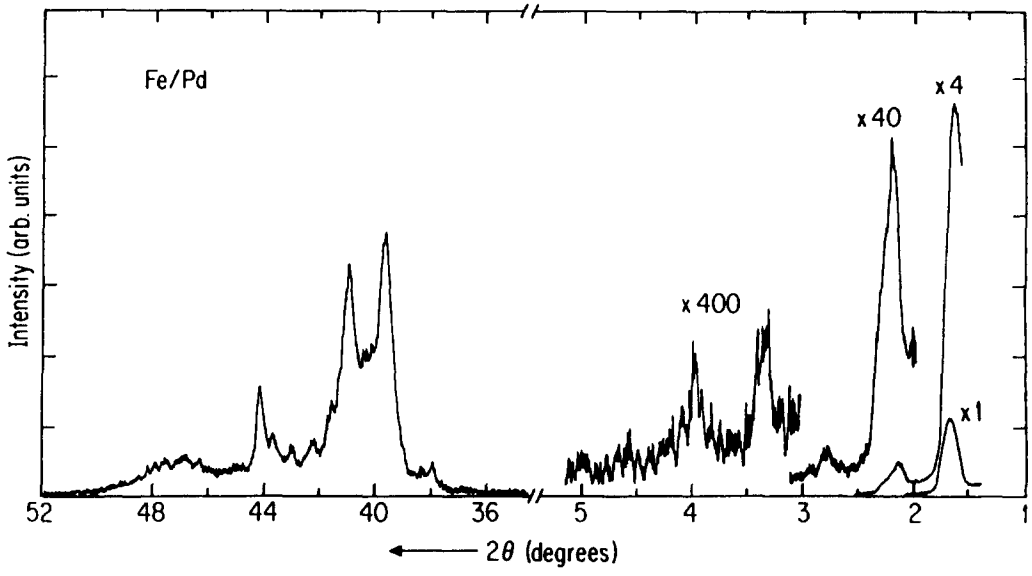

Fig. 1. θ-2θ x-ray diffraction for a second-order Fe/Pd superlattice (sample A) at high and low angles.

Table 1. Input parameters for the calculated reflectances.

	Fe	Pd
$\delta \times 10^6$	22.44	33.29
$k \times 10^6$	2.89	2.85
SAMPLE A		
layer thickness in Λ_1 (Å)	35.5	51.3
layer thickness in Λ_2 (Å)	17.7	25.7
SAMPLE B		
layer thickness in Λ_1 (Å)	23.36	32.96
layer thickness in Λ_2 (Å)	5.84	8.24

certain groups,[10] the agreement between the observed and calculated values is very good.

From high-angle θ-2θ diffraction data, we are able to obtain information on the crystallinity of the samples. We find that Fe/Pd forms a stack of BCC (110) Fe planes on top of FCC (111) Pd planes in the growth direction. The average crystallite size is ~300 Å in the growth direction. We used a wide-film Debye-Scherrer (Read) camera to determine structural information in and out of the growth plane. The exposed films show sharp arcs of length ~15°, which we attribute to the mosaic spread of the crystallites.

Brillouin Scattering

The Brillouin scattering experiments were done in air at room temperature, using a Sandercock-type (3+3)-pass tandem Fabry-Perot interferometer in backscattering geometry. The light source was a single-mode 514.5-mm Ar^+ ion laser with an incident power of

Table 2. Observed and calculated peak positions at low angles.

n	2	3	4	5	6
SAMPLE A					
$2\theta_c$	1.61	2.21	2.85	3.50	4.16
$2\theta_o$	1.62±0.03	2.18±0.03	2.80±0.03	3.37±0.04	4.00±0.04
SAMPLE B					
$2\theta_c$	1.53	2.68	3.89	- -	- -
$2\theta_o$	1.70±0.05	2.60±0.05	3.70±0.05	- -	- -

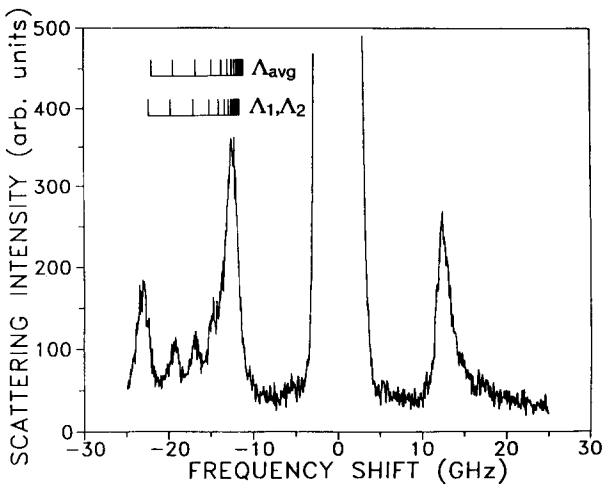

Fig. 2. Typical Brillouin spectrum for Sample B. Also shown are the calculated spin-wave frequencies for a sample of 100 bilayers with Λ_{avg} = 35.2 Å (top) and those of second-order superlattices of 50 bilayers with $\Lambda = \Lambda_1 + \Lambda_2$ = 70.4 Å (Sample B) (bottom).

up to 200 mW at the sample. The inelastically scattered light was depolarized to suppress surface phonon signals. The applied magnetic field of 1 kG was oriented parallel to the layer planes and perpendicular to the scattering plane.

The spin-wave modes of multilayered structures consist of single-layer modes coupled across the interleaving non-magnetic spacer layers.[11-19] The coupling is strongest for dipolar-type (Damon-Eshbach) modes because of their strong stray fields. If the magnetic layers are of equal thickness, the degeneracy of the DE modes is lifted and a so-called collective band of spin-wave excitations is formed.

A typical Brillouin spectrum for these superlattices is shown in Figure 2. The angle of incidence of the laser beam was 45°. Collective spin waves were observed in the region between 12 GHz and 23 GHz. They are identified by their characteristic frequency dependence on the applied magnetic field, as well as the pronounced Stokes/anti-Stokes asymmetry. The asymmetry is smallest for modes at lower frequency shifts, suggesting that in this region the modes are mostly bulk-mode-like. The larger asymmetry at higher frequency shifts shows dominantly surface-mode-like behavior. This result is in agreement with results obtained for conventional superlattices.[17-19] Of the 100 modes theoretically expected for these samples, only the highest three modes can be resolved to within the experimental resolution; the remaining modes form a continuum of collective modes.

We have calculated the spin-wave frequencies using a model described elsewhere, which takes interface anisotropies fully into account.[19] Although this model does not treat exchange contributions, this effect should be small for small bilayer thicknesses.[11] We obtained a very satisfactory agreement between the calculated and the measured spin-wave spectra using the parameters from Ref. 19 for the interface anisotropy constant K_s, -0.15 erg/cm² and the Pd polarization thickness, 0.7 Å. The saturation magnetization was adjusted to 16.5 kG.

For comparison, we calculated the spin-wave frequencies expected of a conventional-type superlattice with 100 bilayers of average modulation wavelength Λ_{avg} = 35.2 Å. The Fe and Pd thicknesses in Λ_{avg} are the averaged Fe and Pd thicknesses of Sample B (Table 1). In the upper left of Figure 2, we show the calculated frequency positions for these first- and second-order superlattices. The obtained frequencies are found to be slightly shifted from each other, demonstrating that the spin-waves frequencies depend on the detailed nature of the modulation of the superlattice. Also, it can be seen that the calculated frequencies for the second-order superlattice fit the experimental data slightly better. By varying the parameters of the calculation, no improvement of the fit could be achieved. The minor differences between the fit and the experimental data presumably are attributable to exchange contributions neglected in the calculations.

Summary

In conclusion, we prepared a new class of metallic superlattices using a stable and reproducible dc sputtering machine. X-ray diffraction analysis of our samples showed reasonable agreement between the calculated and the observed peak positions at low angles. We found that Fe and Pd grow (110) and (111) parallel to the plane of the substrate, respectively. The average crystallite size was ~300 Å. The x-ray diffraction spectra obtained for these second-order superlattices are a unique signature, distinct from first-order (conventional-type) superlattices with the same period.

The experimentally obtained spin-wave frequencies are in good agreement with calculations, taking the full structure of the second-order superlattice into account. A careful analysis showed that the dependence of the spin-wave frequencies on the overall modulation wavelength is stronger than on the ratio of the bilayer thicknesses.

Using this layering scheme for second-order superlattices, it becomes possible to combine very small modulation wavelengths with larger overall modulation wavelengths. This will allow, for example, the study of the influence of interface anisotropies on the formation of perpendicular magnetization in large modulation wavelength superlattices.

Acknowledgement -- This work was supported by the U.S. Department of Energy under contract number DE-FG02-87ER45297, and the Air Force Office for Scientific Research under contract number F49620-86-C-0123. We thank J. A. Leavitt and L. C. McIntyre, Jr. for performing the RBS measurements of our samples.

References

1. For a recent review, see T. Shinjo in *Metallic Superlattices*, T. Shinjo and T. Takada, eds. (Elsevier, Amsterdam, 1987), p. 1.
2. C. M. Falco, J. de Phys. **45**, C5-499 (1984).
3. A. Boufelfel and C. M. Falco, submitted, Appl. Opt.
4. J. A. Leavitt, Nucl. Instr. and Meth. B **24/25**, 717 (1987).
5. B. Vidal and P. Vincent, Appl. Opt. **23**, 1794 (1984).
6. D. B. McWhan, in *Synthetic Modulated Structures*, L. Chang and B.C. Giesen, eds. (Academic, New York, 1985).
7. R. W. James, *The Optical Principles of the Diffraction of X-Rays* (Bell, London, 1948).
8. D. T. Cromer and D. Liberman, J. Chem. Phys. **53**, 1891 (1970).
9. A. Boufelfel, Ph.D. dissertation, University of Arizona, 1988.
10. M. Deutsch and M. Hart, Phys. Rev. B **30**, 640 (1984) and Phys. Rev. B **31**, 3846 (1985).
11. R. E. Camley and D. L. Mills, Phys. Rev. B **27**, 261 (1983).
12. P. Grünberg and K. Mika, Phys. Rev. B **27**, 2955 (1983).
13. P. R. Emtage and M. R. Daniel, Phys. Rev. B **29**, 212 (1984).
14. M. Grimsditch, M. R. Khan, and I. K. Schuller, Phys. Rev. Lett. **51**, 498 (1983).
15. A. Kueny, M. R. Khan, I. K. Schuller, and M. Grimsdich, Phys. Rev. B **29**, 498 (1983).
16. G. Rupp, W. Wettling, W. Jantz, and R. Krishnan, Appl. Phys. A **37**, 73 (1985).
17. B. Hillebrands, P. Baumgart, R. Mock, G. Güntherodt, A. Boufelfel, and C. M. Falco, Phys. R ev. B **34**, 9000 (1986).
18. B. Hillebrands, P. Baumgart, R. Mock, G. Güntherodt, A. Boufelfel, and C. M. Falco, J. Appl. Phys. **61**, 4308 (1987).
19. B. Hillebrands, A. Boufelfel, C. M. Falco, P. Baumgart, G. Güntherodt, E. Zirngiebl, and J. D. Thompson, J. Appl. Phys. **63**(8), 3880 (1988).